

Energy distributions of 1.12-MeV gamma rays Compton scattered by *K*-shell electrons of gold, lead, and thorium*

P. N. Baba Prasad,[†] G. Basavaraju, and P. P. Kane

Department of Physics, Indian Institute of Technology, Powai, Bombay-400076, India

(Received 26 November 1975; revised manuscript received 2 June 1976)

Measurements are reported of the pulse-height distributions of photons of initial energy 1.12 MeV after Compton scattering through 60° and 100° by *K*-shell electrons of Au, Pb, and Th. The energy distributions of scattered photons, obtained in the case of Au and Pb targets by a deconvolution of the detector response function, show a rise for energies lower than about 0.25 MeV, a broadening of the Compton line, and a negligible shift of the Compton peak. On account of natural radioactivity of the Th target, the corresponding pulse-height distributions are not precise enough to make the deconvolution procedure worthwhile. The energy distributions are compared with theoretical calculations based on the nonrelativistic impulse approximation. It is clear that a relativistic calculation incorporating the effects of electron binding in intermediate states is required.

I. INTRODUCTION

The general experimental arrangement and the theoretical background of the present investigation are described in the preceding paper.¹ The energy distributions of γ rays which undergo Compton scattering by the *K*-shell electrons of atoms are required for a complete understanding of this process. A preliminary report on the present work has been presented.²

Important details regarding the present experiment are given in Sec. II. The results and conclusions are presented in Sec. III.

II. EXPERIMENTAL DETAILS

In the present experiment, a fast-slow coincidence system was used with resolving times of 30 nsec and 2 μ sec, respectively. Pulse-height analysis of anode pulses from the γ detector was made with the help of a 20-channel analyzer gated by the output of the coincidence circuit. The linearity of pulse height was checked not only through the singles spectra of the γ rays of different energies but also through the spectra obtained in the coincidence mode. Annihilation quanta from a ²²Na source, and 1.17- and 1.33-MeV γ rays from a ⁶⁰Co source were used for the spectral measurements in the coincidence mode. The photopeaks obtained in the coincidence mode agreed with the positions of the corresponding peaks in the singles spectra. Therefore, useful linearity and gain stability checks could be made more frequently in the singles mode than would have been possible in the coincidence mode. If a check showed a pulse-height shift of more than 2%, the corresponding data were discarded.

Pulse-height distributions of the scattered γ

rays were studied at 60° and 100° scattering angles. In each case, the pulse-height distribution of false events was determined and subtracted from the measured distribution in order to obtain the "true" distribution. In all cases, the chance coincidence rate was less than 1% of the total rate and was considered negligible. The rate in each channel corresponding to N_{eK} of Eq. (2) in the preceding paper was negligible in the case of the high-*Z* targets used here.

For the reasons mentioned in Sec. II of the preceding paper, the distribution of false events was determined with an equivalent aluminum target in the case of targets of thickness less than 30 mg/cm². In the case of the thicker lead targets, an equivalent copper target was also used. A correction had to be made in the case of thorium for its radioactivity. As a result, the errors in the thorium measurements are large.

The "true" pulse-height distributions determined at 60° with lead targets and at 100° with gold and thorium targets are shown in Figs. 1, 2, 3, and 4. In the case of the 143.3 mg/cm² lead target, the "true" distributions corresponding to the subtraction of false events obtained with both aluminum and copper targets are shown in Fig. 1. As mentioned in the preceding paper, the copper-data subtraction technique gives a more reliable determination of the distribution in the case of thick targets. The pulse-height distribution of events corresponding to scattering from free electrons was obtained in the singles mode with an aluminum target. This is shown by the solid line in each figure. With the help of the response function of the detector, it is necessary to deconvolute the pulse-height distribution in order to obtain the energy distribution. The deconvolution procedure is outlined in the Appendix.

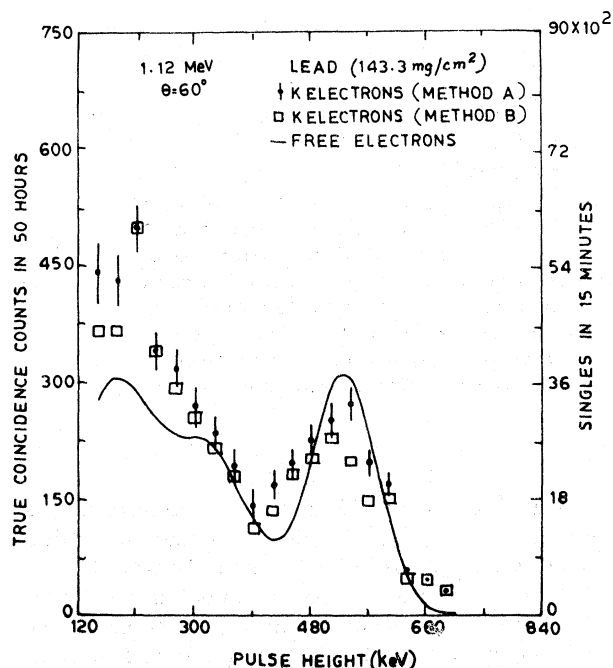


FIG. 1. Pulse-height spectra from 1.12-MeV γ rays which underwent Compton scattering through 60° by K -shell electrons of a 143.3-mg/cm² Pb target. \bullet , K electrons (method A): Coincidence counts in each channel are corrected for false coincidences measured with an equivalent aluminum target. \square , K electrons (method B): Coincidence counts in each channel are corrected for false coincidences measured with an equivalent copper target. The solid line is a smooth curve through the experimental points obtained in the singles mode with a 117.7-mg/cm² aluminum target and represents scattering from free electrons at rest. The errors associated with points on the solid lines in Figs. 1, 2, 3, and 4 are less than 2% except near the highest energies.

III. RESULTS AND CONCLUSIONS

Figures 5 and 6 show the energy distributions of the γ rays Compton scattered at 60° by K -shell electrons of lead of 143.3 and 30.3 mg/cm² thickness, respectively. Figure 7 shows a similar distribution obtained at 100° with a gold target of 12.85 mg/cm² thickness. In view of the poor precision of the data obtained at 100° with thorium, it was not considered worthwhile to perform the elaborate deconvolution procedure in this case. The solid line in each figure represents the measured energy distribution of photons Compton scattered by the electrons of an aluminum target, which can be considered as free and practically at rest. Thus, a direct comparison of the data with the solid line reveals the influence of electron binding. A comparison of the data in Figs. 5 and 6 gives an idea of the distortion introduced by secondary effects associated with thick targets.

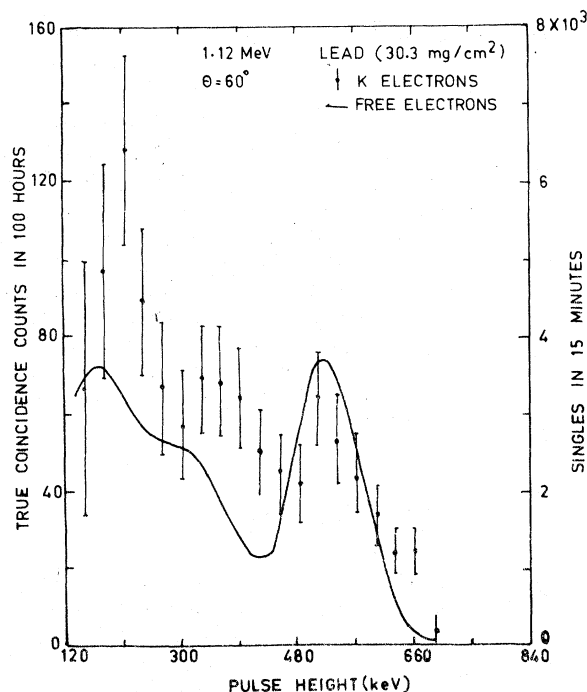


FIG. 2. Pulse-height spectra from 1.12-MeV γ rays which underwent Compton scattering through 60° by K -shell electrons of a 30.3-mg/cm² Pb target (method B). The solid line has the same significance as that in Fig. 1.

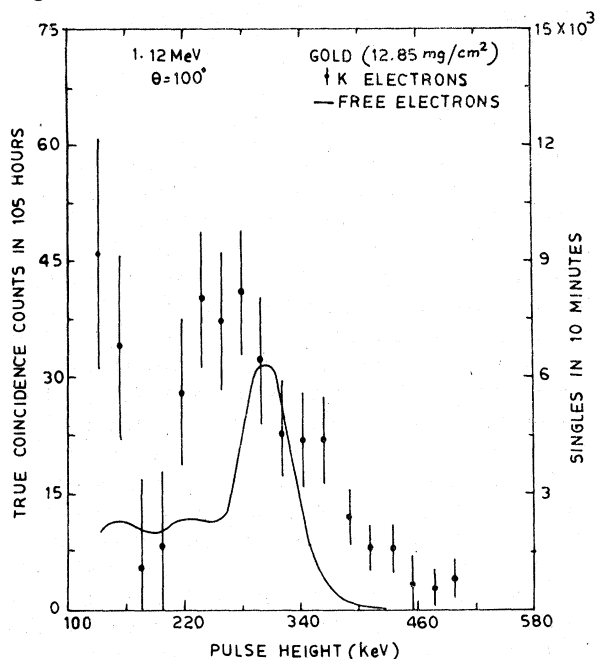


FIG. 3. Pulse-height spectra from 1.12-MeV γ rays which underwent Compton scattering through 100° by K -shell electrons of a 12.85-mg/cm² Au target (method A). The solid line is a smooth curve through the experimental points obtained in the singles mode with a 202.5-mg/cm² Al target and represents scattering from free electrons at rest.

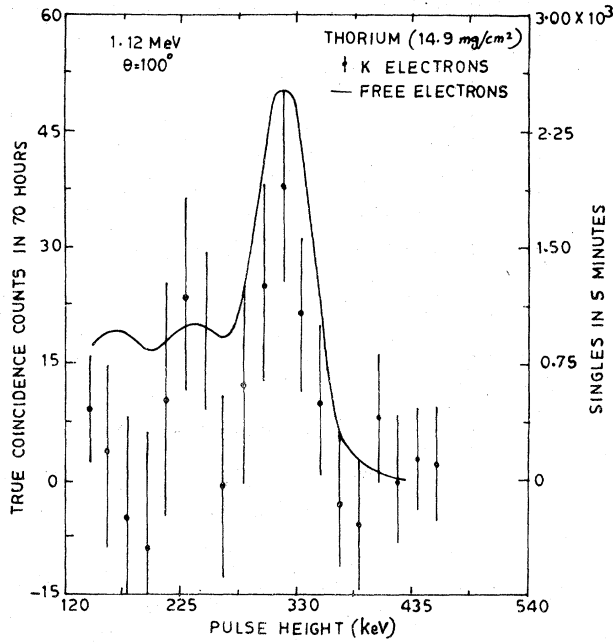


FIG. 4. Pulse-height spectra from 1.12-MeV γ rays having undergone Compton scattering through 100° by K -shell electrons of a 14.9-mg/cm^2 Th target (method A) after an additional correction for false coincidences arising from natural radioactivity of thorium. The solid line has the same significance as that in Fig. 3.

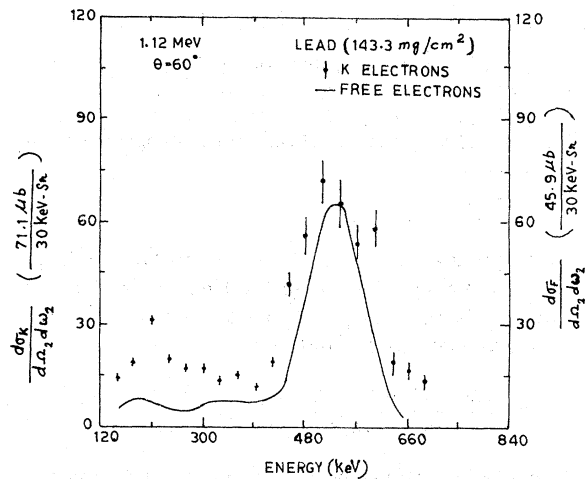


FIG. 5. Experimental values of the differential cross section $d\sigma/d\Omega_2 d\omega_2$ at 60° for a K -shell electron of Pb and a free electron at rest, obtained by a deconvolution procedure from the coincidence data (method B) and the singles data in Fig. 1. A correction for finite angular acceptance has not been applied in Figs. 5, 6, and 7. The data shown here for a very thick Pb target are not compared with theory.

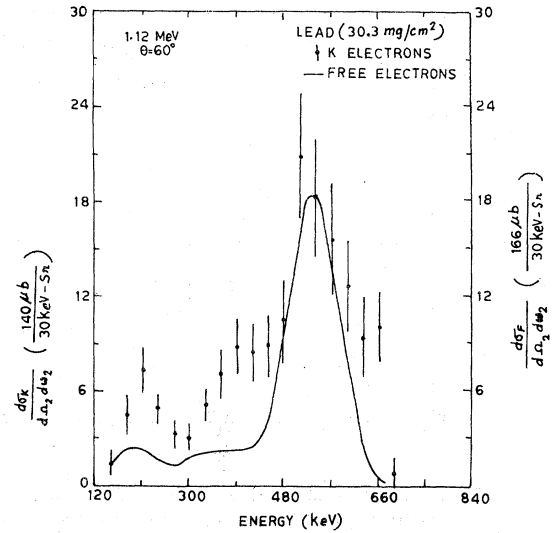


FIG. 6. Experimental values of the differential cross section $d\sigma/d\Omega_2 d\omega_2$ at 60° for a K -shell electron of Pb and a free electron at rest, obtained by a deconvolution procedure from the coincidence data and the singles data in Fig. 2.

There are three prominent characteristics of the energy distributions shown in Figs. 6 and 7. As expected, the distributions extend to photon energies well in excess of that corresponding to the free Compton line. Secondly, the K -electron Compton peaks are broader than the corresponding free-electron peaks. The full width at half-maximum or FWHM of the free-electron peak, ΔE_f , is a measure of the resolution obtained with the sodium-iodide detector under the experimental conditions of angular acceptance.

The values of ΔE_f measured with the help of the solid lines for 60° and 100° are respectively 0.14 ± 0.01 and 0.064 ± 0.007 MeV. These are in good agreement with the corresponding values of about 0.15 and 0.070 MeV, respectively, calculated in a straightforward way from a knowledge of the experimental conditions, the Klein-Nishina formula and the standard Compton expression for scattered photon energy as a function of angle. ΔE_f combines with the FWHM ΔE_K arising from K -shell electron binding and gives rise to the observed FWHM ΔE_0 of the K -shell electron Compton peak. Therefore, we can obtain ΔE_K as $(\Delta E_0^2 - \Delta E_f^2)^{1/2}$. From Figs. 6 and 7, ΔE_K turns out to be approximately 0.18 MeV for lead at 60° and 0.16 MeV for gold at 100° with an error of ± 0.015 MeV. Further, the peak energy in each case is within 0.015 MeV of the free Compton line.

The third prominent feature of the energy distributions in Figs. 6 and 7 is a noticeable increase for scattered photon energies less than about 0.25

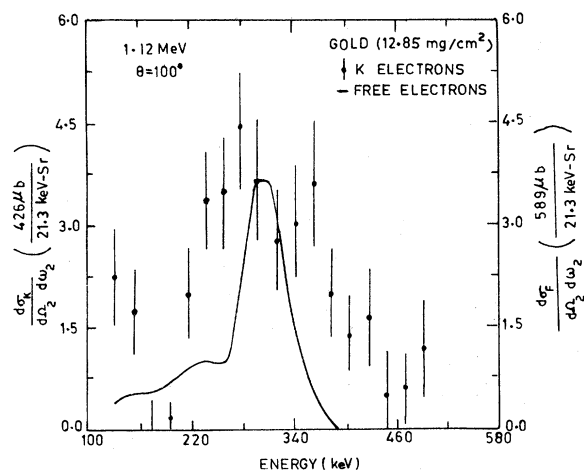


FIG. 7. Experimental values of the differential cross section $d\sigma/d\Omega_2 d\omega_2$ at 100° for a K -shell electron of Au and a free electron at rest, obtained by a deconvolution procedure from the coincidence data and the singles data in Fig. 3.

MeV. The solid line for 60° also shows a small bump at low energies, which almost certainly represents the effect of back scattering. However, this bump is much smaller than the rise observed in the case of the corresponding distribution obtained with lead K -shell electrons. Di Lazzaro and Missoni³ had observed a similar rise in their 0.662-MeV experiment. The $(e/mc)\vec{p}\cdot\vec{A}$ term in the interaction Hamiltonian in the nonrelativistic theory⁴ and $e\vec{\alpha}\cdot\vec{A}$ term in the relativistic formulation^{3,5} lead to the expectation of such a rise which is in fact related to the infrared divergence of quantum electrodynamics. However, if Gavril's method is applied⁶ to 0.662-MeV γ rays, the rise starts only below about 0.060 MeV. Further, the relativistic calculation of Whittingham,⁷ which takes into account electron binding in intermediate states, does not reveal a rise down to 0.1 MeV.

Since calculations of comparable accuracy are not available for 1.12-MeV γ rays, in Fig. 8 we show the results of a nonrelativistic calculation⁶ based on the impulse approximation (IA). It should be noted that this IA calculation does not predict a rise for low energies of the scattered photons. The formula for the K -shell-electron cross-section differential with respect to angle and energy turns out to be as follows:

$$\frac{d\sigma_K}{d\Omega_2 d\omega_2} = \frac{r_0^2(1+\cos^2\theta)}{2} \frac{\omega_2}{\omega_1} \frac{8a^5}{3\pi qc} (a^2 + \xi^2)^{-3}, \quad (1)$$

where r_0 is the classical radius of the electron, θ is the scattering angle, ω_1 and ω_2 are the energies of the incident, and the scattered photons, $d\Omega_2$ is a solid-angle element in the direction of the scat-

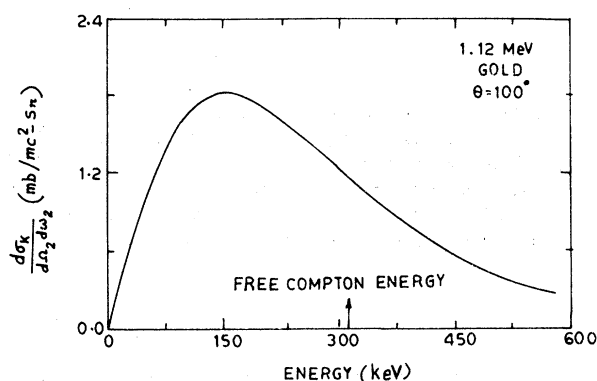
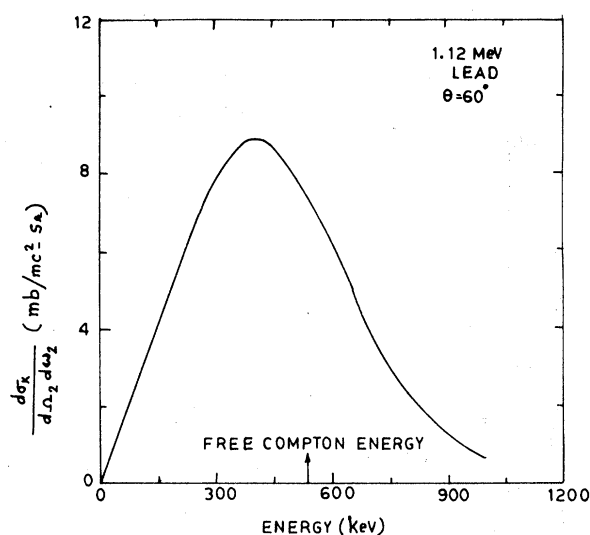


FIG. 8. Theoretical values of the differential cross section $d\sigma/d\Omega_2 d\omega_2$ at 60° for a K -shell electron of Pb and at 100° for a K -shell electron of Au, calculated on the basis of the nonrelativistic impulse approximation (Ref. 6).

tered photon, a is $Z\alpha$, Z is the atomic number of the scattering atom, α is the fine-structure constant, q is the change in photon momentum, and ξ is given by the formula

$$\xi = \left| \frac{\omega_1 - \omega_2}{cq} - \frac{q}{2mc} \right|. \quad (2)$$

The widths calculated with the help of formulas (1) and (2) are 0.33 MeV for gold at 100° and 0.53 MeV for lead at 60° , and are obviously much larger than the experimental values mentioned earlier. The widths calculated with these formulas for 0.662-MeV γ rays are also much larger than those measured by Di Lazzaro and Missoni. The calculations carried out according to nonrelativistic⁸ and relativistic⁹ form-factor treatments also give

widths that are rather large. Further, these calculations do not predict a rise for low energies of the scattered photons.

The peak energies calculated with the help of formulas (1) and (2) are about 0.15 MeV lower than the energies of the free Compton lines at 60° and 100°, obviously in contradiction with the data in Figs. 6 and 7. It is clear that a comprehensive relativistic calculation is required.

ACKNOWLEDGMENT

We are grateful to Professor B. V. Thosar of the Tata Institute of Fundamental Research, Bombay for arranging a loan of the 20-channel pulse-height analyzer.

APPENDIX

A spectral distribution with a certain number $N(E)dE$ of photons in the energy interval dE at E gives rise to a number $n(V)dV$ of pulses with height between V and $V+dV$:

$$n(V)dV = \int_0^{E_{\max}} R(E, V)N(E)dE, \quad (A1)$$

where E_{\max} is the highest photon energy, V is expressed in energy units, and $R(E, V)$ is the response function of the detector. The probability that a photon of energy E generates a pulse of height V is given by $R(E, V)$. With the help of Eq. (A1), $N(E)$ can be obtained from the measured $n(V)$, if $R(E, V)$ is known. The pulse-height distribution was assumed to consist of a Gaussian representing total photon energy absorption and a tail arising from Compton scattering in the detector. The response function $R(E, V)$ can then be written as follows:

$$R(E, V) = \alpha_p g(E, V) + \beta_p \int_0^{T_e^{\max}} C(E, T_e) g(T_e, V) dT_e, \quad (A2)$$

where α_p and β_p represent the probabilities for a photon to produce a pulse in the full energy region and the Compton tail, respectively, $g(E, V)$ is the Gaussian mentioned above, $C(E, T_e)$ is the probability that a photon of energy E produces a Compton electron of energy T_e in the detector, and T_e^{\max} is the maximum energy of a Compton electron;

$$g(E, V) = (s/\sqrt{\pi}) \exp[-s^2(E - V)^2], \quad (A3)$$

where $g(E, V)$ is normalized to unit area and the

full width at half-maximum, W_{FWHM} , of $g(E, V)$ is given by

$$W_{\text{FWHM}} = 1.66/s. \quad (A4)$$

If η is defined as E/mc^2 , T_e^{\max} is given by the relation

$$T_e^{\max} = [2\eta/(1+2\eta)]E. \quad (A5)$$

It has been shown¹⁰ that $C(E, T_e)$ can be written in a normalized form as follows:

$$C(E, T_e) = U \int_0^{T_e^{\max}} U dT_e, \quad (A6)$$

where

$$U = \frac{\pi \gamma_0^2}{\eta^2 m c^2} \left[2 + \left(\frac{T_e}{E - T_e} \right)^2 \times \left(\frac{1}{\eta^2} + \frac{E - T_e}{E} - \frac{2}{\eta} \frac{E - T_e}{T_e} \right) \right]. \quad (A7)$$

If ϵ_B is the detection efficiency of the detector for a γ ray of energy E and p_f is the photofraction, α_p and β_p are respectively equal to $\epsilon_B p_f$ and $\epsilon_B(1 - p_f)$. To determine $R(E, V)$, it is necessary to estimate ϵ_B , p_f , and the FWHM of the Gaussian as a function of E . The detection efficiency ϵ_B was evaluated with the help of standard results.¹¹ The other two quantities were determined experimentally. For this purpose, eight well-known sources of γ rays of energy between 0.122 and 1.12 MeV were used. As a precaution, the geometrical size of each source was the same as that of the targets used during the scattering measurements. The photofraction p_f and the corresponding FWHM were determined from the pulse-height spectrum obtained with each source. Graphs showing the variation of p_f and FWHM with E were plotted. Values of p_f and FWHM at any desired E were obtained by interpolation.

In order to determine $N(E)$, the right-hand side of Eq. (A1) was approximated by a sum

$$n(V_j) \delta V = \delta E \sum_{i=1}^l R(E_i, V_j) N(E_i), \quad (A8)$$

where l is the effective number of channels used to record the pulse-height spectra and δV or δE is the channel width. The index j can take on the values 1 to l . Thus one has to solve a set of l linear equations in order to obtain l values of $N(E_i)$. The final $N(E_i)$ values were converted in a straightforward way to values of $d\sigma/d\Omega_2 d\omega_2$.

*Work supported in part by a grant from the National Bureau of Standards, Washington, D. C. under the PL-480 program.

†Based in part on a thesis submitted by P. N. Baba

Prasad to the Indian Institute of Technology, Bombay.

¹P. P. Kane and P. N. Baba Prasad, preceding paper, Phys. Rev. A 15, 1976 (1977).

²P. N. Baba Prasad, G. Basavaraju, and P. P. Kane,

International Symposium on Radiation Physics, Calcutta, 1974 (unpublished).

- ³M. A. Di Lazzaro and G. Missoni, Istituto Superiore Di Sanita Reports ISS-66/6, 66/7 and 66/8, 1966 (unpublished). Experimental and theoretical work at 0.662 MeV is described here.
- ⁴M. Gavrilu, Phys. Rev. A 6, 1348 (1972); 6, 1360 (1972).
- ⁵L. A. Wittwer, Ph.D. thesis (University of California, Davis, 1972) (unpublished). This report describes calculations for 0.145- and 0.320-MeV γ rays. In this work and the one mentioned in Ref. 3, the contribution of bound intermediate states is not taken into account.
- ⁶H. K. Tseng, M. Gavrilu, and R. H. Pratt, Report No. 2, 1973, prepared at the University of Pittsburgh, Pittsburgh for the National Bureau of Standards (unpublished).
- ⁷I. B. Whittingham, J. Phys. A 4, 21 (1971).
- ⁸F. Schnaidt, Ann. Phys. (Leipz.) 21, 89 (1934).
- ⁹M. Lambert, R. Müller, J. Lang, R. Bösch, and W. Wolfli, Helv. Phys. Acta 39, 355 (1966).
- ¹⁰R. D. Evans, in *Encyclopedia of Physics*, edited by S. Flügge (Springer-Verlag, Berlin, 1958) Vol. 34, p. 267.
- ¹¹W. E. Mott and R. B. Sutton, *ibid.*, Vol. 45, Part 2, pp. 107-109 (1958).